

Development of alkali activated cements and concrete mixture design
with high volumes of red mud

Non Peer-reviewed author version

Krivenko, Pavel; Kovalchuk, Oleksandr; Pasko, Anton; CROYMANS-PLAGHKI, Tom; Hutt, Mikael; Lutter, Guillaume; VANDEVENNE, Niels; SCHREURS, Sonja & SCHROEYERS, Wouter (2017) Development of alkali activated cements and concrete mixture design with high volumes of red mud. In: CONSTRUCTION AND BUILDING MATERIALS, 151, p. 819-826.

DOI: 10.1016/j.conbuildmat.2017.06.031

Handle: <http://hdl.handle.net/1942/24843>

47 by-product. It can be a hazardous material owing to its alkalinity but also because of
48 its enhanced levels of natural occurring radionuclides. A typical plant produces up to
49 twice as much red mud as alumina. Today, over 2.7 billion tons is available worldwide
50 [Liu and Li, 2015]. Disposal costs of red mud can add up to 5% of alumina production
51 costs and it also introduces risks to the environment. Therefore, a lot of effort is
52 dedicated to find suitable applications for use of the large reserves of red mud that are
53 available worldwide. The use of red mud on a large scale in the production of
54 construction materials can be a commercially viable option. Several studies have
55 investigated the application of red mud as an additive for building materials [Sglavo et
56 al, 2000; Hairi, 2015; Pontikes et al, 2007; Tsakiridis, et al, 2004; Pascual et al, 2009;
57 Ye et al, 2014]. In the preparation of special cements from red mud the added quantity
58 of red mud is usually less than 5% [Manfroi et al., 2014; Singh et al., 1997; Pontikes et
59 al, 2007; Tsakiridis et al., 2004]. Alkaline activation allows to considerably increase
60 the quantities of red mud incorporated both in cements and concretes without a
61 decrease of their physico- mechanical characteristics [Pan et al 2003, Pan et al 2002,
62 Ke et al, 2014; Klauber et al, 2011; He et al, 2012; Zhang et al, 2014; Zhang et al,
63 2010; Kumar et al, 2013; Dimas et al, 2009; Hajjajia et al, 2013. Vukcevic et al, 2013;
64 Komnitsas et al, 2009; He et al, 2013 Bošković et al, 2013; Ke et al, 2015]. The
65 limited incorporation levels of red mud can be explained by the fact that such
66 important factors such as the chemical composition of constituent materials, the state
67 of structure and the type of alkaline activator have not been optimized. These factors,
68 according to Glukhovsky (1992) and Krivenko (1985) are important with regard to the
69 formation of alkaline and alkaline- alkali earth phases which eventually determine the
70 properties of the resulting cement stone.

71 An option to use large percentages of red mud is to chemically and thermally
72 convert them to inorganic polymer mortar [Hertel et al., 2016]. The mayor
73 disadvantage of this process is that it is very energy intensive. However, in order to
74 develop an industrially viable option it is crucial to study options for reuse that do not
75 require such an energy intensive pretreatment step.

76 Red mud has a low hydraulic activity. Any cement composition containing red
77 mud should therefore be modified by activating additives, such as amorphous silica,
78 which do not contain calcium. The main goal of the current research is to optimize the
79 formation process of red mud based alkali activated cements. In order to achieve this
80 goal, it is important to control the alkaline medium (alkalinity) and the presence of
81 oxides, such as CaO , Al_2O_3 , SiO_2 , Fe_2O_3 and others in the active form. The alkalinity
82 and oxides are required for synthesis of proper hydration products—mineral substances
83 of alkaline aluminosilicate composition. As a rule, these substances act as structure-
84 forming elements not only during the formation of solid rocks in nature, but in ancient
85 concretes as well. Analcime, an alkaline aluminosilicate hydrate composed of Na_2O
86 Al_2O_3 SiO_2 H_2O , is formed in ancient cements and acts as a so-called "eternal" bond.
87 Specific features of ancient cements, distinguishing them from contemporary Portland
88 cements, are the high contents of amphoteric (Al_2O_3 and Fe_2O_3), acid (SiO_2) and alkali
89 metal oxides (Na_2O and K_2O). It is therefore worthwhile to investigate to which extent
90 red muds containing large quantities of amphoteric oxides. Fe_2O_3 and Al_2O_3 (over
91 60%) could be used as components of the alkali activated cements in long term
92 applications.

93 More and more attention is paid to the presence of naturally occurring
94 radionuclides in building materials. According to the CPR (Construction Products
95 Regulation) the construction works must be designed and built in such a way that
96 emission of dangerous radiation will not be a threat to health of occupants or
97 neighbors. A unified legislation across the Member States of the European Union will
98 come into act in February 2018 i.e. the Euratom Basic Safety Standards (EU-BSS,
99 [CE-2014]). According to this legislation building materials incorporating naturally
100 occurring radioactive materials (NORM), such as red mud, require a radiological
101 screening before approved use as building materials. Red muds can contain enhanced
102 concentrations of naturally occurring radionuclides [Somlai et al, 2008;Nuccetelli et
103 al., 2015].

104 In this study different mixture designs were formulated that enable the
105 incorporation of high percentages of red mud in cement and concrete. To assure safe
106 application of red mud in the different considered mixtures, the radiological properties
107 of the constituents and the resulting construction materials are investigated.
108

109 2. Materials and methods

110 2.1 Constituents

111 Concrete and cement specimens (d= 50 mm; h= 25 mm) with various
112 incorporation rates of bauxite residue were prepared. The chemical composition of the
113 main constituent materials used in the concrete and cement specimens are given in
114 Table 1.

115 A Ukrainian red mud of the following mineralogical composition (% by mass):
116 25-27% hematite, 25-28% goethite, 4.5-6.5% rutile and anatase, 15-17% hydrogarnets,
117 6-7% sodium aluminosilicate hydrate, 2.5-3.0% calcite was used in the experiments in
118 cements and concretes.

119 Blast-furnace slag and Ordinary Portland Cement (OPC) were used to introduce
120 aluminosilicate components varying in basicity, expressed by a basicity
121 modulus $\left(M_b = \frac{CaO + MgO}{SiO_2 + Al_2O_3} \right)$, and content of glass phase (80% for GGBFS and 5%
122 for OPC measured by XRD analysis) in order to regulate the structure formation
123 processes.

124 All solid cement constituents excluding alkalis were jointly ground until a
125 fineness of 350-450 m²/kg (specific surface by Blaine).

126 Sodium silicate (Ms=2.8; p=1300 kg/m³); soda ash (Na₂CO₃) and sodium
127 metasilicate pentahydrate (Na₂O·SiO₂·5H₂O) were used as alkaline components.

128 Local river sand with maximum grain size of 1.2 mm, granite aggregate with
129 fractions 5-10 mm and 5-20 mm, granite screenings (fr. 2.5-5 mm) and red mud with
130 particle sizes varying from 50 to 1000 μm were used as aggregates for concretes.
131

132 **Table 1**
 133 Chemical composition of constituent materials

Cement components	Oxides, % by mass									
	SiO ₂	Al ₂ O ₃	MnO	Fe ₂ O ₃	CaO	MgO	TiO ₂	R ₂ O	M _b	Glass content
Red mud	4.8	12.9	-	48.6	10.1	-	5.3	2.5	-	-
Ground Granulated blast-furnace slag (ggbs)	37.9	6.85	0.106	-	44.6	5.21	0.35	-	1.0	80
OPC	23.4	5.17	-	4.12	64.13	0.88	-	-	2.27	5

134
 135 **2.2 High volume red mud alkali activated cements**
 136

137 Different compositions of red mud, ground granulated blast-furnace slag (glassy
 138 additive) and OPC (high-basic calcium containing additive) were mixed with soda ash,
 139 sodium metasilicate and soluble sodium silicate as alkaline components in order to
 140 produce alkali activated cements. An overview of the compositions of the produced
 141 alkali activated cements is given in Table 2.
 142

143 **Table 2**
 144 Compositions of alkali activated cements containing red mud

Composition	Red mud, % by mass	ggbs, % by mass	OPC, % by mass
Alkaline component: soda ash (Na ₂ CO ₃)(5% by mass of ggbs + red mud)			
K1	50	50	-
K2	60	30	10
K3	70	30	-
K4	70	20	10
K5	80	15	5
Alkaline component: sodium metasilicate (Na ₂ SiO ₃)(5% by mass of ggbs + red mud)			
K6	50	50	-
K7	70	25	5
Alkaline component: soluble sodium silicate (Ms=2.8, ρ=1400 kg/m ³) (soluble sodium silicate/ggbs + red mud=0.4)			
K8	50	50	-
Alkaline component: soluble sodium silicate (Ms=2.8, ρ=1300 kg/m ³) (soluble sodium silicate/ggbs + red mud=0.4)			
K9	60	30	10
K10	50	50	-

145
 146 **2.3 Red mud containing concretes**
 147

148 Different concentrations of red mud were used as fine aggregate in alkali
 149 activated cement concretes. For the concrete mixes given in table 3, fine aggregate –
 sand – was substituted for up to 38.6% (by mass) bauxite red mud.

150
151
152
153

Table 3

Characteristics of high volume red mud alkali activated cement concretes (quantities of red mud– up to 38.6% by mass of dry constituents)

No	Cement components, (kg)			Aggregates, (kg)	
	ggbs	OPC	alkaline component	crushed stone (fraction)	red mud
C1	536	14	soluble sodium silicate ($\rho=1400 \text{ kg /m}^3$, $M_s=2.8$), 308	800 (5-20)	850
C2	536	14	soluble sodium silicate ($\rho=1400 \text{ kg /m}^3$, $M_s=2.6$), 460	200 (5-10) 200 (screenings)	850

154
155
156
157
158
159

The concrete products listed in Table 4 are manufactured by pressing.

Table 4

Mix design of pressed (press stress $P= 30 \text{ MPa}$) concrete road bases with various incorporation rates of red mud

No	Concrete mixture design, % by mass				
	Cement, % by mass			Aggregates, % by mass	
	ggbs	Na_2CO_3	$\text{Na}_2\text{SiO}_3 \cdot 5\text{H}_2\text{O}$	red mud	sand (fr. finer than 0.63 mm)
CRB1	13.8	0.6	0.6	85	-
CRB2	13.8	0.6	0.6	65	20
CRB3	13.8	0.6	0.6	45	40
CRB4	9.2	0.4	0.4	90	-

160
161
162
163
164
165
166
167
168
169
170
171
172
173
174
175
176
177

2.4 Methods for physico- mechanical analysis

Physico- mechanical properties of the formulated cements were studied following the Ukrainian national standard DSTU B.V 2.7-181:2009 “Alkaline cements. Specifications”. In the preparation of the concretes the Ukrainian national standard DSTU - N B.V.2.7-304:2015 “Manual on the manufacture and use of alkaline cements, concretes and structures” was followed. Specimens were allowed to harden in normal conditions.

Hydration products of the formulated cements were studied using a set of physico- chemical examination techniques, such as X-ray phase diffractometry, differential-thermal analysis (DTA), thermogravimetry and electron microscopy. X-ray phase diffraction analysis was done using diffractometers DRON-3M and DRON-4-07 with a copper tube at voltage=30 kV, current=10-20 mA and angle range $2\theta = 10-60^\circ$ at a speed of counter rotation= 2° per minute. Differential- thermal and thermogravimetric analyses were carried out using an instrument of the system F.Paulik, J.Paulik, L.Erdey (company MOM, Budapest, Hungary). The specimens were heated at a speed of 10°C per minute until a temperature of 1000°C was reached. Scanning electron microscopy (SEM) was carried out using scanning electron microscope

178 equipped with microanalyzers REMMA-102-02 (resolving power in the regime of
179 secondary electrons is no more than 5 nm, magnification range is X10400000, a range
180 of accelerating voltage of 0.2- 40 kV is used, maximum excessive pressure in the
181 electron column is $6.7 \cdot 10^{-4}$ Pa).

182 Softening coefficient of material was calculated as a ratio between compressive
183 strength after saturation in water for 2 days and compressive strength of reference
184 material (not saturated). The material is water resistant if the softening coefficient is
185 more than 0.8 [DSTU B A.1.1-5-94].
186

187 2.5 Method for radiological evaluation

188 The gamma-ray spectrometry measurements were performed on a HPGe-
189 detector of the Radionuclide Metrology Laboratory of JRC-Geel in Belgium. The
190 detector is located in the 225 m deep underground laboratory Hades located on the
191 premises of the Belgian Nuclear Centre SCK•CEN in Mol, Belgium. The crystal has a
192 planar configuration and a small point contact (so-called BEGe-detector). The relative
193 efficiency is 19% and FWHM of 1.23 keV and 1.64 keV at respectively 661.6 keV and
194 1332 keV. It has a submicron top dead layer. The shielding is composed of 5 cm
195 copper + 15 cm lead. The background count rate of the detector is 220 counts per day
196 in the energy interval 40 to 2700 keV. All samples were dried at 110°C until constant
197 mass was reached. Then they were placed in radon-tight Teflon containers and stored
198 for at least 21 days before starting a measurement (to establish secular equilibrium
199 between ^{226}Ra and daughters). The samples were placed directly on the endcap. The
200 sample masses were 94.92 g, 134.74 g, 114.18 g and 138.85 g for ggbs, sand, OPC and
201 red mud respectively. The measurement times varied between 7 and 17 days and the
202 deadtime was always below 1%. All the activity concentrations are reported with the
203 measurement date as reference date, which was between 395 and 440 days after the
204 sampling date. No decay correction to the sampling date was made.

205 An activity concentration index (ACI_{SP}) for streets and playgrounds (Equation
206 1) that uses the activity concentrations of ^{226}Ra , ^{232}Th , ^{40}K and ^{137}Cs has been defined
207 by Markkanen (1995),
208

$$209 \quad ACI_{SP} = \frac{Ac_{226Ra}}{700 \frac{Bq}{kg}} + \frac{Ac_{232Th}}{500 \frac{Bq}{kg}} + \frac{Ac_{40K}}{8000 \frac{Bq}{kg}} + \frac{Ac_{137Cs}}{2000} \quad (1)$$

210
211 with Ac being the activity concentration of the mentioned radionuclide expressed in
212 Bq/kg.

213 Note that an ACI_{SP} index value above 1 indicates an effective gamma dose
214 larger than 0.1 mSv/a. The activity concentration index proposed by the EU-BSS could
215 not be used in this case, since it was defined for evaluation of building materials and
216 not for road construction.

217 In this study, the used activity concentration of ^{232}Th is the activity
218 concentration of ^{228}Ac and the activity concentration of ^{226}Ra is the weighted mean
219 between the activity concentrations of ^{214}Pb and ^{214}Bi . The ^{40}K and ^{137}Cs activity
220 concentrations were measured directly using their respective gamma emission lines at
221 1460.8 keV and 661.6 keV.

222 Equation 2 is used for the calculation of the uncertainty (u) on the ACI_{SP}.
223

$$u(ACI_{SP}) = \sqrt{\left(\frac{1}{700}\right)^2 u^2(AC_{226Ra}) + \left(\frac{1}{500}\right)^2 u^2(AC_{232Th}) + \left(\frac{1}{8000}\right)^2 u^2(AC_{40K}) + \left(\frac{1}{2000}\right)^2 u^2(AC_{137Cs})}$$

224
225 (2)
226

227 With u(AC_{226Ra}) being the uncertainty on the activity concentration of the mentioned
228 radionuclide.

229 Following Radiation Protection 122 (RP-122 part II, Chapter 4.2.6) dose
230 assessments of road construction workers were performed such that it considers the
231 occupational exposure linked to the use of concrete containing red mud. In this work,
232 the NIRS (Japanese National institute on Radiological Sciences) dose assessment tool
233 was used for the dose assessments calculations [NIRS website].

234 The activity concentration (in this paper meaning the activity per unit of mass)
235 was determined by dividing the final activity determined for each radionuclide by the
236 measured dry mass of the sample. The used methodology regarding the data analysis
237 (data acquisition, spectrum analysis, full peak efficiency calculation), dose assessment
238 and calculation of the ACI_{SP} is described in more detail in by Croymans et al. (2016).
239

240 3. Results and discussion

241 Several steps are undertaken for a systematic investigation of the use of high volume
242 fractions of red mud in alkali activated cements and concretes:

243 (1) Firstly, the concept that enables the compositional buildup of alkali activated
244 cement, using a high volume fraction of red mud, is proposed and a proof of concept is
245 given.

246 (2) Secondly, the role of red mud in the structure formation of hardened cement paste
247 is investigated in detail.

248 (3) Thirdly, the use of red mud as an aggregated in concrete for road base is evaluated.

249 (4) Finally, the radiological properties of the synthesized alkali activated cements and
250 concretes are evaluated.
251

252 3.1 Concept for compositional buildup of alkali activated cement

253 The process of hydration and hardening can be considered as a complex process
254 involving (1st stage) destruction-coagulation, (2nd stage) coagulation-condensation and
255 (3rd stage) condensation-crystallization [Glukhovsky, 1994]. It was demonstrated that
256 the quantity of glass phase is a determining factor at the 1st stage of the processes of
257 hydration and hardening [Krivenko, 1985]. Crystalline high-basic calcium silicates
258 quickly hydrate in alkaline medium promoting acceleration of the 3rd stage because of
259 their hydration products. These calcium silicates can act as crystallo-chemical
260 intensifiers of hardening. Absence of these crystalline phases in the initial material
261 retards the 3rd stage of the structure formation process.

262 The role played by anions originating from alkaline component is a double one
263 and is determined by the anion type. Anions can be divided into two groups: (1) anions
264 that enter into cement within soluble silicates and aluminates and (2) anions that can
265 be found in all remaining alkaline compounds. The anions of the first group are similar

266 to the hydrated primary destruction products of the aluminum-silicon-oxygen
267 framework in the solid phase (SiOH), they serve as a reserve for the hydrated primary
268 destruction products and, naturally, are the most effective anions in terms of hydration
269 and structure formation. Anions of the second group change the properties of the liquid
270 phase, and some participate in the formation of complexes which extract the
271 destruction products into a solid phase promoting intensification of the hydration
272 processes [Krivenko, 1985].

273 Thus, a compositional buildup of high volume red mud alkali activated cements
274 should be based on a proper choice of the optimal ratio of red mud (with additives of
275 glassy structure) to high-basic additives which quickly hydrate and crystallize in
276 highly alkaline media [Krivenko, 1996, Rostovskaya, 1994].

277 In order to verify this concept in practice, a mixture of cement components
278 containing 60% (by mass) ground bauxite red mud, 30% (by mass) granulated blast-
279 furnace slag (glassy additive) and 10% (by mass) OPC (high-basic calcium containing
280 additive) (K9 in Table 2), was mixed with soluble sodium silicate ($M_s=2.8$;
281 $p=1300 \text{ kg/m}^3$). For the sodium silicate solution, the liquid to solid ratio was 0.4. The
282 strength of the prepared cement-sand mortar (1:3) specimens was 6.25 MPa after 2
283 days of normal hardening (temperature $20\pm 2^\circ\text{C}$ and relative humidity $95\pm 4\%$), 30 MPa
284 after 7 days and 60 MPa after 28 days demonstrating that this concept can be used.

285

286 **3.2 Role of red mud in the microstructure formation of hardened cement paste**

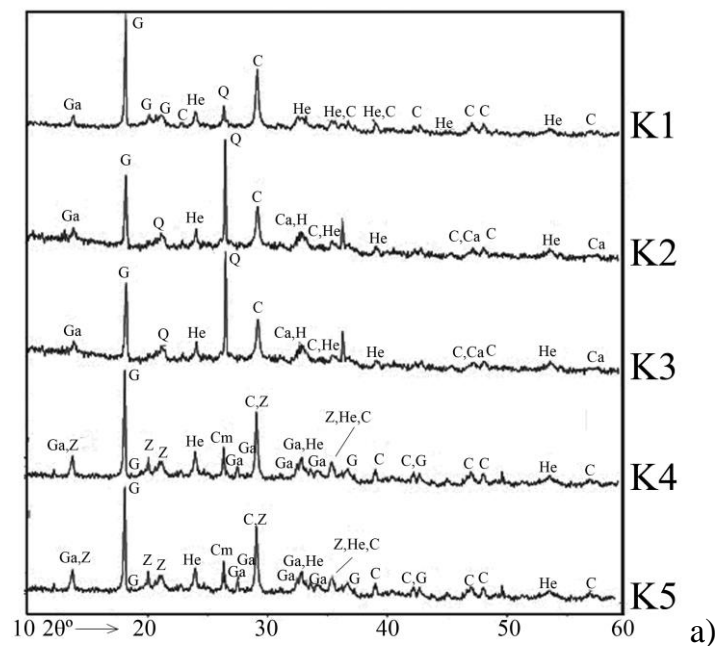
287 For the determination of the microstructure of the hardened cement paste the
288 compositions in Table 2 were used. The role of red mud in the microstructure
289 formation was investigated when using (1) soda ash, (2) sodium metasilicate and (3)
290 sodium silicate as alkaline components.

291 The determination of the phase composition of hydration products of the
292 formulated cements was not straightforward. This can be explained, from one side, by
293 a multi-component composition of cementitious systems themselves, and from the
294 other side, by the fact that each individual component is also a complex system (red
295 mud, slag and cement). In some cases, this resulted in a superposition of characteristic
296 responses making identification of the hydration products more complicated.

297 The results of X-ray phase diffraction analysis (Figure 1a) of the cements K1-
298 K5 (Table 2) in which soda ash was used as alkaline component showed that hydration
299 products were represented mainly by tri-calcium aluminates $3\text{CaO}\cdot\text{Al}_2\text{O}_3$ (diffraction
300 characteristics 0.272; 0.191; 0.161, PDF#330251) and calcite CaCO_3 (0.368; 0.262;
301 0.228; 0.209; 0.191; 0.188, PDF#721937). The higher contents of the red mud in the
302 cement composition (K5 and K4) resulted in the formation of zemkorite $\text{Na}_2\text{Ca}(\text{CO}_3)_2$
303 (0.639; 0.438; 0.425; 0.303, PDF#411440) and gaylussite $\text{Na}_2\text{Ca}(\text{CO}_3)_2\cdot 5\text{H}_2\text{O}$ (0.639;
304 0.270; 0.272; 0.321, PDF#210343). The addition of OPC (up to 10%) (K2, K4, and
305 K5) was found to accelerate mineral formation processes at the early stages of
306 hardening and improves the formation of a crystalline structure for the resulted cement
307 stone.

308 In case of sodium metasilicate use (Figure 1b), the phase composition is
309 somewhat different. The following minerals are formed: klinoferrosilite FeSiO_3
310 (0.643; 0.335; 0.321; 0.304; 0.260, PDF#821832) and lawsonite $\text{CaAl}_2[\text{Si}_2\text{O}_7]$
311 $(\text{OH})_2\cdot\text{H}_2\text{O}$ (0.487; 0.417; 0.368; 0.273, PDF#771994). When going to higher contents

312 of the red mud from 50 to 70% (K6 and K7) the structure formation process
 313 decelerates, though it does not stop completely. This means that the red mud takes an
 314 active part in cement hydration processes. The formation of clinoferrrosilite in the
 315 hydration products supports the assumption that hematite contained in large quantities
 316 in the red mud takes part, provides the condition of an alkaline medium, in the
 317 formation of hydration products. The use of soluble sodium silicate (K8) as alkaline
 318 component considerably accelerates the formation of calcium silicate hydrates and is a
 319 basement of crystallization processes in the cement. Soluble sodium silicate enters
 320 actively into interaction with red mud and calcium-containing additive. In the case of
 321 compositions with lower density of soluble glass (K9, K10) the prevailing hydration
 322 products are found to be tri-calcium aluminates $3\text{CaO}\cdot\text{Al}_2\text{O}_3$ (0.272; 0.191; 0.161,
 323 PDF#330251), calcites CaCO_3 (0.368; 0.262; 0.228; 0.209; 0.191; 0.188,
 324 PDF#411440) and crystals of hematite (PDF#850599).



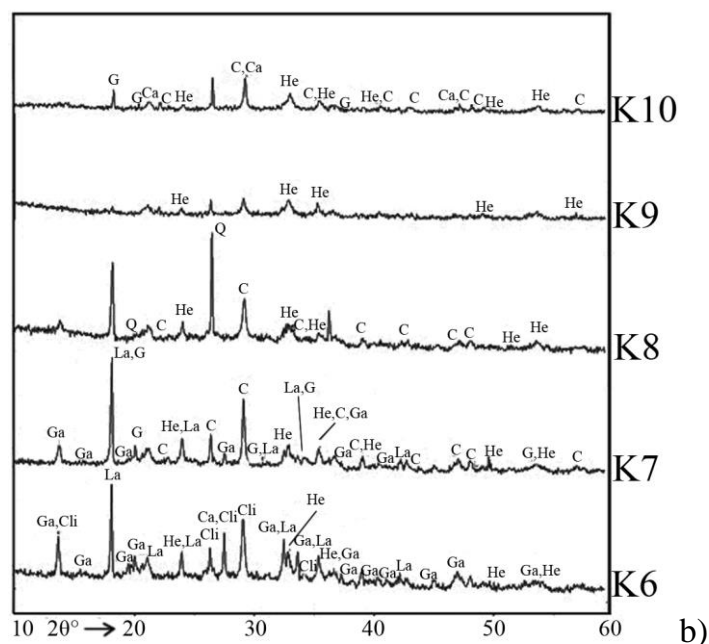


Fig.1. X-ray phase diffraction patterns of a cement stone from the alkali activated cements containing red mud and alkaline component: a – soda ash; b – soluble sodium silicate + sodium metasilicate. Designation: He – hematite (Fe_2O_3), Ca - $\text{Ca}_3\text{Al}_2\text{O}_6$ – tri-calcium aluminat ($3\text{CaO}\cdot\text{Al}_2\text{O}_3$), C – CaCO_3 – calcite, Q – (SiO_2) quartzite, G – gibbsite ($\text{Al}(\text{OH})_3$), Z – zemkorite ($\text{Na}_2\text{Ca}(\text{CO}_3)_2$), Ga – gaylussite ($\text{Na}_2\text{Ca}(\text{CO}_3)_2\cdot 5\text{H}_2\text{O}$), Cm – caminite ($(\text{MgSO}_4)_2\cdot(\text{OH})_2$), Cli – klinoferrosilite (FeSiO_3), La – lawsonite ($\text{CaAl}_2[\text{Si}_2\text{O}_7](\text{OH})_2\cdot\text{H}_2\text{O}$)

325
326
327
328
329
330
331
332
333

The obtained results coincide well with the results of DTA. At temperatures between 270 and 350°C an endothermic effect takes place as a result of loss by gibbsite of OH^- groups. The occurrence of tri-calcium aluminat is confirmed by heat adsorption at 740°C (Figure 2) [Gorshkov at al., 1981]. A wide endothermic band in the DTA curve between 390 and 700°C gives an indication of the release of constitutional water with break of hydrogen bonds.

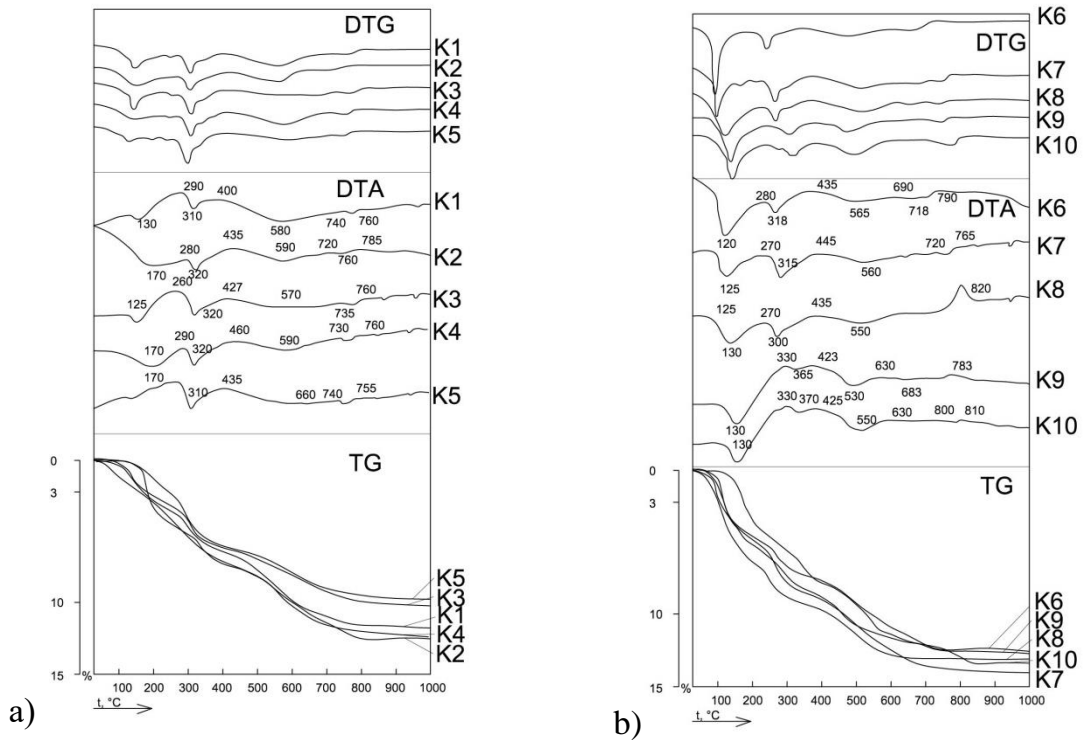


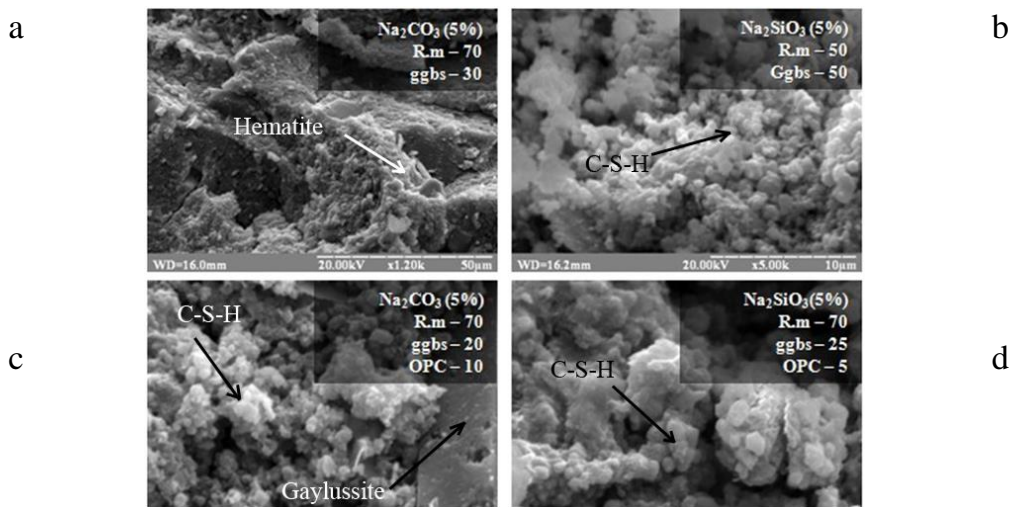
Fig. 2. DTA curves of a cement stone from alkali activated cement containing red mud and alkaline components: a – soda ash; b – soluble sodium silicate + sodium metasilicate

334

335 Electron microscopy studies of the cleavage surface of a cement stone from the
 336 alkali activated cement in case of soda ash as alkaline component showed the presence
 337 of calcium silicate hydrates, crystals of gaylussite (Ref
 338 to:<https://www.mindat.org/min-1662.html>) and particles of hematite (Ref
 339 to:<https://www.mindat.org/min-1856.html>) (Figure 3a, c). Photos taken of the cleavage
 340 surface case of sodium metasilicate, showed the formation of calcium silicate hydrates
 341 (Figure 3 b, d).

342 A cleavage surface featured a dense character without cracks, testifying to a
 343 uniform flow of the structure formation processes.

344



345 **Fig.3.** SEM images of the alkali activated cements with incorporated red mud, a – K3,
346 b – K6, c – K4, d – K7

347
348

349 In case of soluble sodium silicate as alkaline component, the quantity of
350 calcium silicate hydrates tends to increase considerably, testifying to a more active
351 interaction of the components owing to the use of alkaline components with the higher
352 silicate modulus.

353 At the same time, the formation of a gel-like phase of alkaline ferro-
354 aluminosilicate hydrates could not be excluded [Locher F.W.]

355

356 **3.3 High volume red mud alkali activated concrete mix design**

357 Incorporation of red mud into alkali activated cement compositions, even in
358 quantities reaching 60% by mass of the cement, will only lead to 14.5% by mass of red
359 mud in the final product – concrete, under the assumption of a cement content of 500
360 kg/m³.

361 In order to increase the quantity of the incorporated bauxite residue, the red
362 mud in a state “as produced” can be used as fine aggregates in making the alkali
363 activated cement concretes. This type of concretes was produced and the concrete mix
364 design is given in Table 3. Increasing of red mud content in the concrete mix (Table 3)
365 to almost 40% by mass of concrete constituents leads to some problems at early stages
366 of hardening. However, optimization of aggregate composition made it possible to
367 have a good strength (over 20 MPa) even after 1 day. Results of the concrete test are
368 given in Table 5.

369 Substitution of fine aggregate – sand – to up to 38.6% by mass red mud allows
370 producing rather high-slump concretes with high strength reaching 70.8 MPa after 28
371 days (Table 5). Incorporation of even higher mass percentages of red mud in concrete
372 mixtures can create technical difficulties because of its (red muds) high water demand
373 as a result of the high fineness characteristic of red mud. The water content does not
374 affect the concrete strength characteristics, however, it influences the performance
375 properties of the resulted concretes leading to a lower freeze-thaw- and corrosion
376 resistance.

377

378 **Table 5**

379 Characteristics of high volume red mud alkali activated cement concretes (quantities
380 of red mud– reaching up to 38.6% by mass of dry constituents)

No	Slump (mm)	Compressive strength, (MPa), age		
		1 day	7 days	28 days
C1	170	13.72	43.57	63.5
C2	110	22.89	49.81	70.8

381

382 To tackle the issue of water demand, a possibility to utilize red mud in
383 quantities in excess of 35% (by mass) is to use them in concrete products

384 manufactured by pressing (moisture content is 8-16% by mass).By means of pressing
 385 large percentages, up to 90% by mass, of red mud can be used when considering them
 386 for application in road base. The mix design of such materials is given in Table 4.
 387 Results of the study are given in Table 6.

388

389 **Table 6** Characteristics of pressed (P= 30 MPa) concrete road bases with various
 390 incorporation rates of red mud

No	Water, % by mass over 100%	Density , kg/m ³	Compressive strength after 7 days, MPa
CRB1	15	2036	5.10
CRB2	14	2121	9.15
CRB3	12	2125	12.5
CRB4	16	2092	4.09

391

392 As is demonstrated by Table 6, even after seven days of hardening in normal
 393 conditions, the strength of the concrete was larger than 3.5 MPa, as is required for
 394 compressive strength of concrete road bases. Testing for water resistance showed that
 395 the specimen CRB 1, after 7 days of hardening in normal conditions and following 2
 396 days of saturation with water, had a softening coefficient of 0.88 while specimen CRB
 397 4 had a softening coefficient of 1.02. In this way, it is demonstrated that the materials
 398 are water resistant and from the technical point of view they could be used as a basis
 399 for road construction even when red mud incorporation is 90% by mass.

400

401 3.4 Radiological characterization

402 3.4.1 Radiological characterization of raw materials

403 In Table 7 the measured activity concentrations of the individual radionuclides
 404 in the main constituents of the red mud containing cements and concretes are given.
 405 The Minimum Detectable Activity (MDA) was determined using the decision
 406 threshold as defined in the standard ISO11929:2010.

407

408 **Table 7**

409 Measured activity concentrations in Bq/kg (dry weight) of individual gamma emitting
 410 radionuclides from the main constituents of the red mud containing concretes (k=2).

Sample	²³⁸ U series					²³⁵ U
	²³⁴ Th	^{234m} Pa	²¹⁴ Pb	²¹⁴ Bi	²¹⁰ Pb	²³⁵ U
Red mud	83 ± 17	84 ± 11	75 ± 5	73 ± 5	91 ± 19	3.5 ± 0.4
ggbs	103 ± 17	98 ± 13	99 ± 6	96 ± 6	<5	4.6 ± 0.4
OPC	36 ± 6	33 ± 5	32 ± 2	30 ± 2	22 ± 6	1.6 ± 0.2
Sand	2.6 ± 1.1	<10	3.0 ± 0.2	3.0 ± 0.3	2.9 ± 0.8	0.18 ± 0.04

Sample	²³² Th series					⁴⁰ K
	²²⁸ Ac	²²⁴ Ra	²¹² Pb	²¹² Bi	²⁰⁸ Tl	⁴⁰ K
Red mud	191 ± 12	188 ± 13	192 ± 13	189 ± 20	193 ± 12	39 ± 4
ggbs	52 ± 4	53 ± 4	52 ± 4	49 ± 9	52 ± 4	119 ± 11
OPC	19.4 ± 1.5	18.5 ± 1.5	19.2 ± 1.3	18.0 ± 3.2	18.9 ± 2.0	231 ± 20
Sand	2.7 ± 0.3	2.8 ± 0.5	2.8 ± 0.2	<4	2.7 ± 0.3	64 ± 6

411

412

413

414

415

416

417

418

419

420

421

422

423

424

425

426

427

428

429

430

431

432

433

434

435

436

437

438

439

440

441

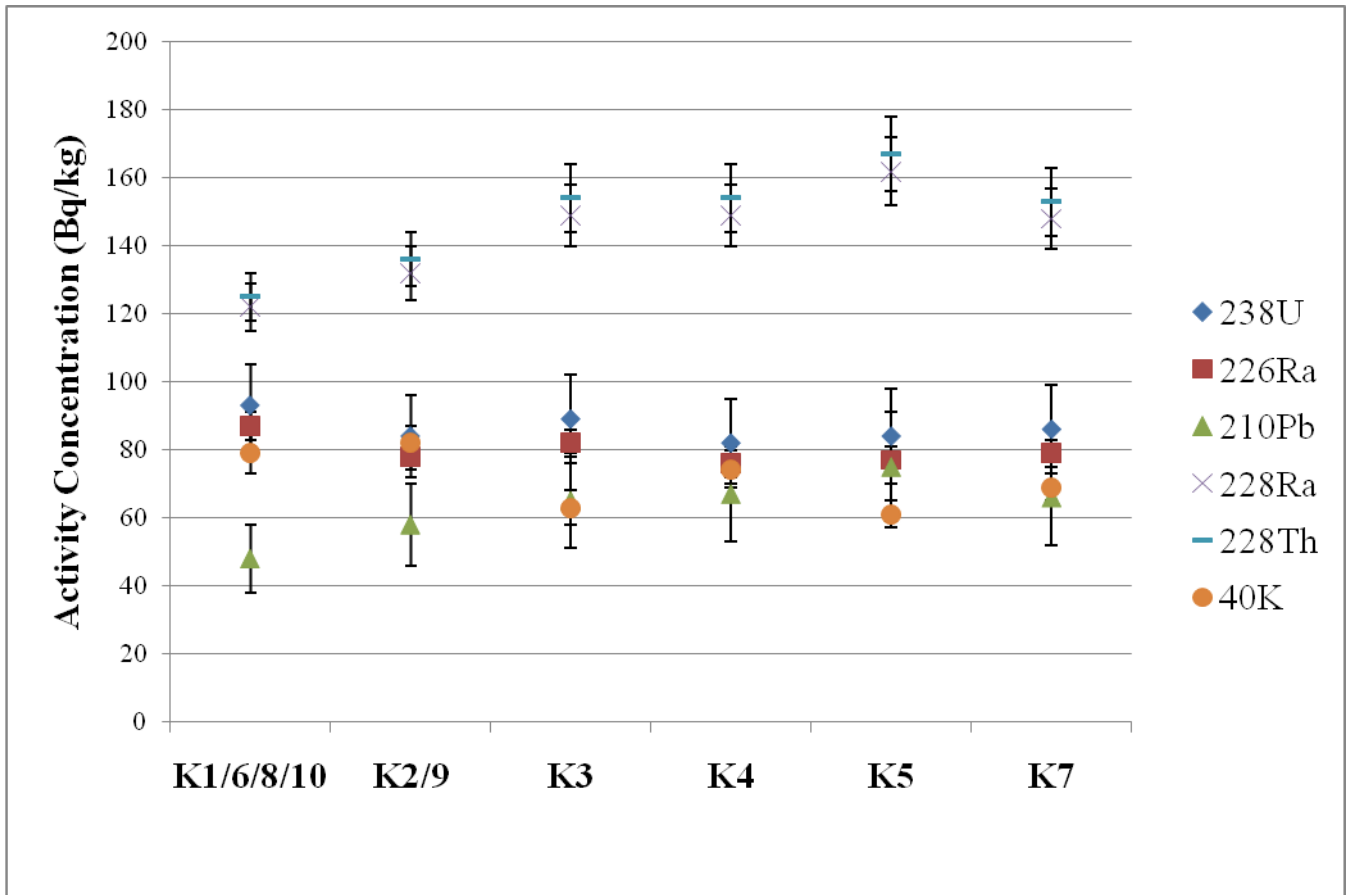
442

As we expect natural isotopic abundance, the values for ²³⁵U could be considered merely as a quality control tool. The activity ratio of ²³⁸U/²³⁵U is consistent within uncertainties with the expected value of 21.6 for all samples. When considering the ²³⁸U decay chain from ²³⁸U to ²¹⁴Bi, the activity concentrations of the different radionuclides in ggbs are comparable or slightly higher in comparison to the same radionuclides in red mud (Table 7). The situation is different for ²¹⁰Pb. For ggbs, there is no secular equilibrium anymore between ²¹⁰Pb and the other radionuclides in the ²³⁸U series whilst for red mud the equilibrium between ²³⁸U down to ²¹⁰Pb is maintained. Considering the production process of metallurgical slags, like ggbs, it is reported in literature that the presence of volatile elements such as Pb is limited in the slag fraction [Croymans et al. 2017; European commission, 1997; Vanmarcke et al., 2003]. The activity concentrations of both red mud and ggbs are 20-40 times higher than sand and 2-4 times higher than OPC for the measured radionuclides in the ²³⁸U decay chain (when not taking into account ²¹⁰Pb). Secular equilibrium is observed for both OPC and sand.

For the ²³²Th series, secular equilibrium is apparent from all the measured activity concentrations of the individual radionuclides in all four sample types (Table 7). The measured activity concentrations for the individual radionuclides in red mud are in this case approximately a factor 3.5 higher than the activity concentrations of the same radionuclides in ggbs. For ⁴⁰K the activity concentration for ggbs is a factor 3 higher than for red mud. When compared to sand, the activity concentrations of the radionuclides from the ²³²Th decay chain are approximately 70 and 19 times higher respectively for red mud and ggbs. In comparison to OPC, the activity concentrations of respectively red mud and ggbs are approximately a factor 10 and 3 higher for the ²³²Th decay chain.

¹³⁷Cs was not found in any of the samples and the MDA was in all cases below 1 Bq/kg.

3.4.2 Radiological evaluation of alkali activated cement pastes



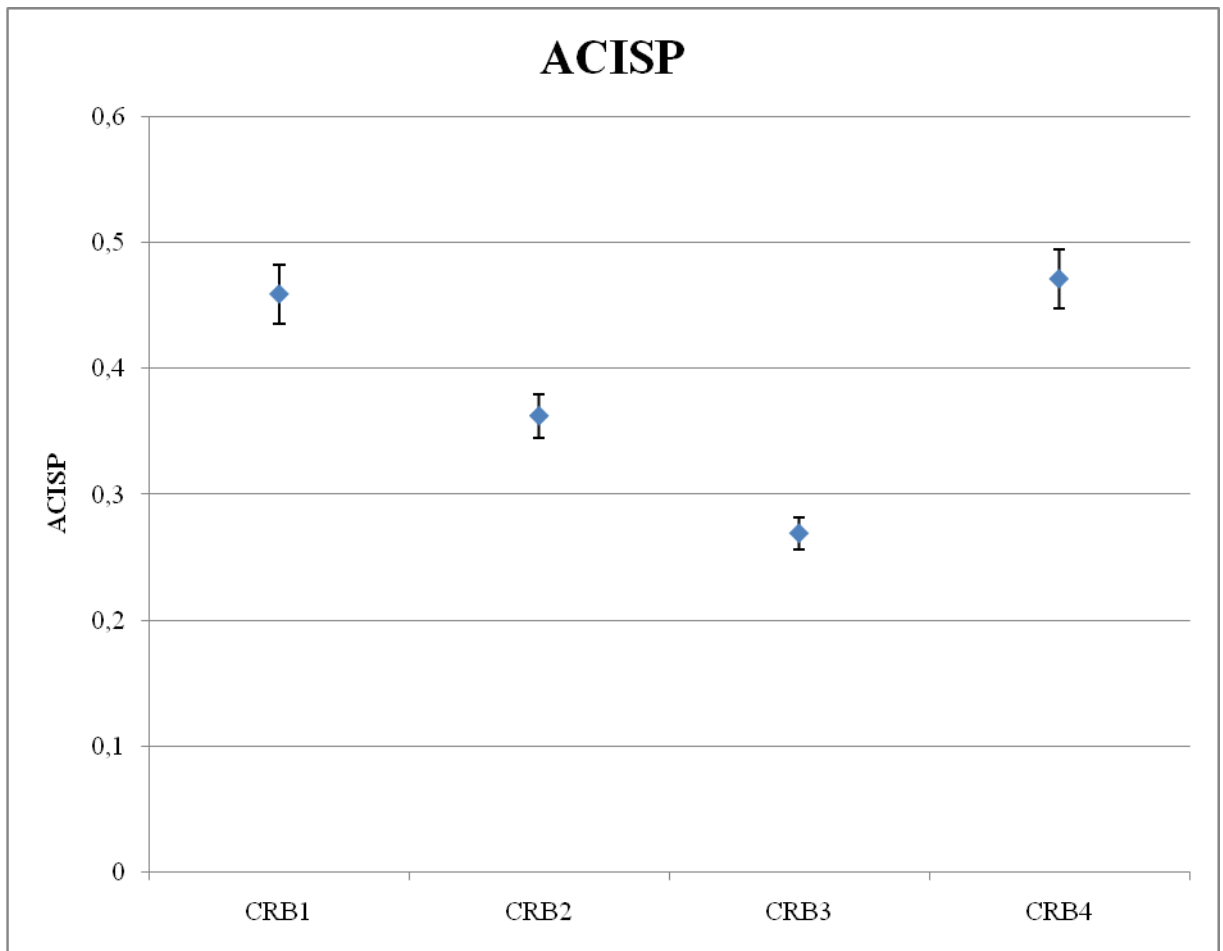
443
 444 **Fig. 4.** Activity concentrations of the produced cements that were calculated on the
 445 basis of the measured activity concentrations of the constituents considering the
 446 composition in Table 2.

447
 448
 449 In Figure 4 the activity concentrations for the newly produced cements
 450 (composition in Table 2), calculated from the constituents, are given. For all the
 451 cements the activity concentrations of the considered radionuclides of the ²³⁸U and
 452 ²³²Th decay series and ⁴⁰K are well below the exemption/clearance levels of the EU-
 453 BSS of 1 kBq/kg and 10 kBq/kg.

454
 455

456
457

3.4.3 Radiological evaluation of alkali activated concretes for road construction



458
459
460
461
462

Fig. 5. ACI_{SP} calculated for the produced concretes on the basis of the measured activity concentrations of the constituents considering the composition in Table 4.

463
464
465
466
467
468
469
470
471
472

The public and occupation exposure linked to the use of the prepared concrete mixtures (Table 4) for road base was verified. Figure 5 shows that all calculated ACI_{SP} -values were below 1. So the external gamma dose for public exposure is lower than the 0.1 mSv/y dose threshold level proposed by Markkanen. The assessment of occupational exposure for workers - via the RP-122 part II “Road construction” scenario - was calculated for samples of Table 4. The calculated total doses to the road construction workers are 0.22 ± 0.02 ; 0.18 ± 0.02 ; 0.13 ± 0.01 and 0.23 ± 0.063 mSv/y for respectively CBR1, CBR2, CBR3 and CBR4. These values are below the 0.3 mSv/y dose threshold level proposed by RP-122 [European Commission, 2001].

473
474
475
476

4. Conclusions

The alkali activated cements with red mud incorporation reaching 80% by mass as well as concrete mixtures for road construction with incorporation rates reaching 90% by mass have been designed and tested. Compressive strength of cements could

477 reach up to 60 MPa and compressive strength of concrete could be up to 70 MPa
478 depending on composition and technology.

479 Main hydration products explaining the high performance properties are: low-
480 basic calcium silicate hydrates (CSH) and alkaline ferro- and aluminosilicate
481 (klinoferrosilite FeSiO_3 , lawsonite $\text{CaAl}_2[\text{Si}_2\text{O}_7](\text{OH})_2 \cdot \text{H}_2\text{O}$).

482 From the radiological point of view all materials under study are able to be used
483 for road construction, even when red mud incorporation reaches 90% by mass.

484

485 **Acknowledgements**

486 The authors would like to acknowledge networking support by the COST Action
487 TU1301 (www.norm4building.org). This work was supported by the European
488 Commission within HORIZON2020 via the EURATOM project EUFRAT for
489 transnational access. The technical support of Gerd Marissens and Heiko Stroh is
490 gratefully acknowledged.

491

492

493 **References**

- 494 • Bošković, I., Vukčević, M., Krgović, M., Ivanović M., Zejak, R. (2013), The
495 influence of raw mixture and activators characteristics on red mud based
496 geopolymers, *Research Journal of Chemistry and environment*, 17:34-40.
- 497 • CE - Council of the European Union, 2014. Council Directive
498 2013/59/EURATOM of 5 December 2013 laying down basic safety standards
499 for protection against the dangers arising from exposure to ionizing radiation,
500 and repealing Directives 89/618/Euratom, 90/641/Euratom, 96/29/Euratom,
501 97/43/Euratom and 2003/122/Euratom. *Off. J. Eur. Union L 13*, 1e73,
502 17.1.2014.
- 503 • Croymans, T., Schroeyers, W., Krivenko, P., Kovalchuk, O., Pasko, A., Hult,
504 M., Marissens, G., Lutter, G., Schreurs, S. (2017), Radiological characterization
505 and evaluation of high volume bauxite residue alkali activated concretes,
506 *Journal of Environmental Radioactivity*, 168: 21-29.
- 507 • Croymans, T., Vandael-Schreurs, I., S., Hult, M., Marissens, G., Stroh, H.,
508 Lutter, G., Schreurs, S. Schroeyers, W. (2017), Variation of natural
509 radionuclides in non-ferrous fayalite slags during a one-month production
510 period, *J. Environ. Radioact.*, 172:63–73.
- 511 • Dimas, D.D.; Giannopoulou, I.P.; Panias, D. (2009), Utilization of alumina red
512 mud for synthesis of inorganic polymeric materials. *Mineral Processing and
513 Extractive Metallurgy Review: An International Journal*, 30:211-239.
- 514 • DSTU BA.1.1-5-94. General physical and technical characteristics and
515 exploitation properties of building materials. Terms and definitions. (Ukrainian
516 National Standard).
- 517 • European Commission (1997), Materials containing natural radionuclides in
518 enhanced concentrations - Report EUR 17625.
- 519 • European Commission (2001), Radiation protection 122 practical use of the
520 concepts of clearance and exemption Part II application of the concepts of
521 exemption and clearance to natural radiation sources.

- 522 • Glukhovskiy, V. (1994), Ancient, Modern and Future Concretes, First Inter.
523 Conf. Alkaline Cements and Concretes. Ukraine, Kiev 1:1-8.
- 524 • Glukhovskiy V.D. (1992), Selected works. Budivelnik, Kiev, Ukraine.
- 525 • Hairi, S.N.Md, Jameson, G.N.L., Rogers, J.J., MacKenzie, K.J.D. (2015),
526 Synthesis and properties of inorganic polymers (geopolymers) derived from
527 Bayer process residue (red mud) and bauxite, *J.Mater. Sci.* 50: 7713-7724.
- 528 • Gorshkov, V.S., Timashev V.V, Saveliev, V.G. (1981), Methods of chemical
529 analysis of binders. Moscow
- 530 • Hajjajia W., Andrejkovičová A., Zanellic C., Alshaaerd M., Dondic M.,
531 Labrinchab J.A., Rochaa F. (2013), Composition and technological properties
532 of geopolymers based on metakaolin and red mud. *Materials & Design*, 52:648-
533 654.
- 534 • He J., Zhang Z., Yu Y., Zhang G. (2012), The strength and microstructure of
535 two geopolymers derived from metakaolin and red mud-fly ash admixture: A
536 comparative study. *Construction and Building Materials*, 30:80-91.
- 537 • He J, Jie Y, Zhang Z, Yu Y, Zhang G (2013), Synthesis and characterization of
538 red mud and rice husk ash-based geopolymer composites. *Cement and Concrete*
539 *Composites*, 37:108-118.
- 540 • Hertel, T., Blanpain, B. & Pontikes, Y. (2016), A Proposal for a 100 % Use of
541 Bauxite Residue Towards Inorganic Polymer Mortar, *J. Sustain. Metall.*, 2
542 (4):394-404
- 543 • Ke, X., Ye, N., Bernal, S.A., Provis J.L., Yang, J. (2014), Preparation of one-
544 part geopolymer from thermal alkali activated bauxite red mud. *Proc. Second*
545 *Int. Conf. on Advances in Chemically-activated Materials*. June 1-3, Changshi,
546 P.R.China, 204– 211.
- 547 • Ke, X, Bernal S.A., Ye, N, Provis, L.J., Yang, J. (2015), One-Part Geopolymers
548 Based on Thermally Treated Red Mud/NaOH Blends. *J Am Ceram Soc*, 98:5-
549 11.
- 550 • Klauber, C., Gräfe, M., Power G. (2011), Bauxite residue issues: II. options for
551 residue utilization. *Hydrometallurgy*, 108:11-32
- 552 • Komnitsas K, Zaharaki D (2009), Utilization of low-calcium slags to improve
553 the strength and durability of geopolymers. *Geopolymers: Structures,*
554 *Processing, Properties and Industrial Applications*. Woodhead, Cambridge,
555 p.353.
- 556 • Krivenko P.V., (1985), Synthesis of Binders with Required Properties in the
557 system $Me_2O-MeO-MeO_3-SiO_2-H_2O$. DSc(Eng.) Thesis, Kyiv, (in Ukraine)
- 558 • Kumar, A., Kumar, S. (2013), Development of paving blocks from synergistic
559 use of red mud and fly ash using geopolymerization. *Construction and Building*
560 *Materials*, 38:865-871.
- 561 • Liu, Z., Li, H. (2015), Metallurgical process for valuable elements recovery
562 from red mud—A review, *Hydrometallurgy*, 155: 29-43
- 563 • Locher, F.W. (2006), *Cement. Principles of production and use*. Dusseldorf,
- 564 • Manfroi, E.P., Cheriaf, M., Rocha, J.C. (2014), Microstructure, mineralogy and
565 environmental evaluation of cementitious composites produced with red mud
566 waste. *Constr. Build. Mater.*, 67, 29–36 (Part A).

- 567
- 568
- 569
- 570
- 571
- 572
- 573
- 574
- 575
- 576
- 577
- 578
- 579
- 580
- 581
- 582
- 583
- 584
- 585
- 586
- 587
- 588
- 589
- 590
- 591
- 592
- 593
- 594
- 595
- 596
- 597
- 598
- 599
- 600
- 601
- 602
- 603
- 604
- 605
- 606
- 607
- 608
- 609
- 610
- 611
- Markkanen, M. (1995), Radiation dose assessments for materials with elevated natural radioactivity. STUK-B-STO 32, Helsinki 1995. 25 p. + app. 13 p.
 - NIRS database; NIRS, NORM database Research Center for radiation protection – National institute of radiological sciences. http://www.nirs.go.jp/db/anzendb/NORMDB/ENG/1_datasyousai.php consulted in March and April 2016
 - Nuccetelli, C., Pontikes, Y., Leonardi, F., Trevisi, R. (2015), New perspectives and issues arising from the introduction of (NORM) residues in building materials: a critical assessment on the radiological behaviour. *Construction and Building Materials*, 82:323-331.
 - Pan, Z., Dongxu, L., Jian, Y., Naunu, Y. (2003), Properties and microstructure of the hardened alkali-activated bauxite red mud slag cementitious material. *Cement and Concretes Research*, 33:1437– 1441.
 - Pan, Z., Dongxu, L., Jian, Y., Nanru, Y. (2002), Hydration products of alkali-activated slag-bauxite red mud cementitious materials. *Cement and Concretes Research*, 32:357– 362.
 - Pascual, J., Corpas, F., Lopez-Beceiro, J., Benitez-Guerrero, M., Artiaga, R. (2009), Thermal characterization of a Spanish bauxite red mud. *Journal of Thermal Analysis and Calorimetry*, 96(2):407– 412.
 - Patent of Ukraine UA 10286 A, Krivenko P., Petropavlovsky O. Rostovskaya G., C 04 B7/06, 7/06, 25.12.96, Bulletin No 4.
 - Pontikes, Y., Nikolopoulos, P., and Angelopoulos, G.N. (2007), Thermal behavior of clay mixtures with bauxite residue for the production of heavy clay ceramics. *Journal of the European Ceramic Society*, 27:1645–1649.
 - Power, G., Grafe, M., and Klauber, C. (2009), Review of current bauxite residue management, disposal and storage: practices, engineering and science. CSIRO Document DMR-3608:3–4
 - Rostovskaya, G.S. (1994), Alkaline binders based on bauxite residues. *First Int. Conference on Alkaline Cements and Concretes*, Kyiv, Ukraine, 1:329-346.
 - Sglavo, V.M., Maurina, S., Conci, A., Salviati, A., Carturan, G., Cocco, G. (2000), Bauxite red mud in the ceramic industry Part 2: Production of clay-based ceramics. *Journal of the European Ceramic Society*, 20:245–252.
 - Singh, M., Upadhyay, S.N., Prasad, P.M. (1997), Preparation of iron rich cements using red mud. *Cem. Concr. Res.*, 27(7):1037–1046.
 - Somlai, J., Jobbágy, V., Kovács, J., Tarján, S., Kovács, T. (2008), Radiological aspects of the usability of red mud as building material additive. *Journal of Hazardous Materials*, 150(11):541-545
 - Tsakiridis, P.E., Agatzini-Leonardou, S., and Oustadakis, P. (2004), Bauxite red mud addition in the raw meal for the production of Portland cement clinker. *Journal of Hazardous Materials*, 116:103– 110.
 - Vanmarcke, H., Paridaens, J., Froment, P. (2003), Overzicht van de NORM-problematiek in de Belgische industrie. (in Dutch)
 - Vukcevic, M., Turovic, D., Krgovic, M., Boscovic, I., Ivanovic, M., Zejak, R. (2013), Utilisation of Geopolymerisation For obtaining Construction Materials Based on Red Mud. *Mater Technol*, 47:99-104.

- 612
- 613
- 614
- 615
- 616
- 617
- 618
- 619
- 620
- 621
- Ye, N., Yang, J., Ke, X., Zhu, J., Li, Y., Xiang, C., Wang, H., Li, L., Xiao, B. (2014), Synthesis and characterization of geopolymer from Bayer red mud with thermal pretreatment. *J Am Ceram Soc*, 97:1652–1660.
 - Zhang, G., He, J. and Gambrell, R.P. (2010), Synthesis, Characterization, and Mechanical Properties of Red Mud-Based Geopolymers, *Transportation Research Record: Journal of the Transportation Research Board*, 2167:1-9.
 - Zhang, M., El-Korchi, T., Zhang, G., Liang, J., Mingjiang, T. (2014), Synthesis factors affecting mechanical properties, microstructure, and chemical composition of red mud–fly ash based geopolymers., *Fuel*, 134:315-325.